



UNIVERSITY OF LEEDS

This is a repository copy of *Organics Substantially Reduce HO₂ Uptake Onto Aerosols Containing Transition Metal ions*.

White Rose Research Online URL for this paper:
<http://eprints.whiterose.ac.uk/91314/>

Version: Accepted Version

Article:

Lakey, PSJ, George, IJ, Baeza-Romero, MT et al. (2 more authors) (2016) *Organics Substantially Reduce HO₂ Uptake Onto Aerosols Containing Transition Metal ions*. *Journal of Physical Chemistry A*, 120 (9). pp. 1421-1430. ISSN 1089-5639

<https://doi.org/10.1021/acs.jpca.5b06316>

Reuse

Unless indicated otherwise, fulltext items are protected by copyright with all rights reserved. The copyright exception in section 29 of the Copyright, Designs and Patents Act 1988 allows the making of a single copy solely for the purpose of non-commercial research or private study within the limits of fair dealing. The publisher or other rights-holder may allow further reproduction and re-use of this version - refer to the White Rose Research Online record for this item. Where records identify the publisher as the copyright holder, users can verify any specific terms of use on the publisher's website.

Takedown

If you consider content in White Rose Research Online to be in breach of UK law, please notify us by emailing eprints@whiterose.ac.uk including the URL of the record and the reason for the withdrawal request.



eprints@whiterose.ac.uk
<https://eprints.whiterose.ac.uk/>

1 **Organics Substantially Reduce HO₂ Uptake Onto Aerosols Containing**
2 **Transition Metal ions**

3
4 Pascale S. J. Lakey¹⁺, Ingrid J. George², Maria T. Baeza-Romero³, Lisa K. Whalley^{1,4} and
5 Dwayne E. Heard^{1,4,*}

6
7 ¹ *School of Chemistry, University of Leeds, Woodhouse Lane, Leeds, LS2 9JT, UK*

8 ² *Now at National Risk Management Research Laboratory, U.S. Environmental Protection*
9 *Agency, T.W. Alexander Drive, Research Triangle Park, NC 27711, USA*

10 ³ *Escuela de Ingeniería Industrial de Toledo, Universidad de Castilla la Mancha, Avenida*
11 *Carlos III s/n Real Fábrica de Armas, Toledo, 45071, Spain*

12 ⁴ *National Centre for Atmospheric Chemistry, University of Leeds, Woodhouse Lane, Leeds,*
13 *LS2 9JT, UK*

14
15
16
17 * *Corresponding author: d.e.heard@leeds.ac.uk*

18 *+ 44 (0) 113 343 6471 (tel)*

19 *+44 (0) 113 343 6401 (fax)*

20
21
22
23 *+ née Matthews, now at Max-Planck-Institut für Chemie, Hahn-Meitner-Weg 1, 55128 Mainz,*
24 *Germany*

25

26

27

28 **Abstract**

29

30 A HO₂ mass accommodation coefficient of $\alpha = 0.23 \pm 0.07$ was measured onto sub-micron
31 copper (II) doped ammonium sulphate aerosols at a relative humidity of $60 \pm 3 \%$, at 293 ± 2
32 K and at an initial HO₂ concentration of $\sim 1 \times 10^9$ molecule cm⁻³ using an aerosol flow tube
33 coupled to a sensitive Fluorescence Assay by Gas Expansion (FAGE) HO₂ detection system.
34 The effect upon the HO₂ uptake coefficient γ of adding different organic species (malonic acid,
35 citric acid, 1,2 diaminoethane, tartronic acid, ethylenediaminetetraacetic acid (EDTA) and
36 oxalic acid) into the copper (II) doped aerosols was investigated. The HO₂ uptake coefficient
37 decreased steadily from the mass accommodation value to $\gamma = 0.008 \pm 0.009$ when EDTA was
38 added in a one-to-one molar ratio with the copper (II) ions, and to $\gamma = 0.003 \pm 0.004$ when
39 oxalic acid was added into the aerosol in a ten-to-one molar ratio with the copper (II). EDTA
40 binds strongly to copper (II) ions potentially making them unavailable for catalytic destruction
41 of HO₂, and could also be acting as a surfactant or changing the viscosity of the aerosol. The
42 addition of oxalic acid to the aerosol potentially forms low-volatility copper-oxalate complexes
43 that reduce the uptake of HO₂ either by changing the viscosity of the aerosol or causing
44 precipitation out of the aerosol forming a coating. It is likely that there is a high enough oxalate
45 to copper (II) ion ratio in many types of atmospheric aerosols to decrease the HO₂ uptake
46 coefficient. No observable change in the HO₂ uptake coefficient was measured when the other
47 organic species (malonic acid, citric acid, 1,2 diaminoethane and tartronic acid) were added in
48 a ten-to-one molar ratio with the copper (II) ions.

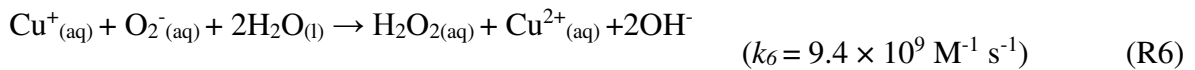
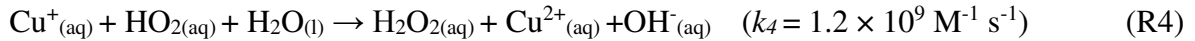
49

50 Introduction

51

52 OH and HO₂ radicals play vital roles in atmospheric chemistry by controlling the oxidative
 53 capacity of the troposphere, with HO₂ acting as a short-lived reservoir for OH and a source of
 54 ozone in more polluted environments via its reaction with NO. Several field studies have
 55 observed significantly lower concentrations of HO₂ radicals than predicted using box models,
 56 and HO₂ loss onto aerosols was suggested as a possible missing sink¹⁻¹⁷. For many of these
 57 field measurements, for example during the ARCTAS campaign in the Arctic and the Rishiri
 58 Island field campaign, the HO₂ uptake coefficient was estimated as 1, which is the maximum
 59 possible^{7, 9}. However, of the relatively few laboratory studies measuring HO₂ uptake
 60 coefficients onto aerosols, it has been shown that the HO₂ uptake coefficient is only equal to
 61 the mass accommodation for aerosols containing elevated copper ion concentrations (~ 0.3 –
 62 0.4 M)¹⁸⁻²¹. The mechanism for the catalytic destruction of HO₂ in the presence of copper ions
 63 is shown below²².

64



(aq)

65

66 It has previously been calculated that a typical copper ion concentration within aerosols in rural
 67 regions was $\sim 2.9 \times 10^{-3} \text{ M}$ ^{23, 24}. This estimation was based upon the measured aerosol size
 68 distributions in rural areas and a soluble copper concentration of 3.1 ng m⁻³ measured at a site
 69 in central Sweden²⁴. Thornton et al.²⁵ developed an expression that allowed the HO₂ uptake
 70 coefficient to be predicted based upon the copper ion concentration within the aerosol, as
 71 shown below:

$$\frac{1}{\gamma^{\text{HO}_2}} = \frac{1}{\alpha^{\text{HO}_2}} + \frac{w}{H_{\text{eff}} RT \sqrt{k^I D_{\text{aq}} Q}} \quad (\text{E1})$$

72 where γ^{HO_2} is the uptake coefficient of HO₂, α_{HO_2} is the mass accommodation coefficient, w is
 73 the molecular thermal speed of HO₂, H_{eff} is the effective Henry's law constant, R is the universal
 74 gas constant, T is the temperature, k^I is the pseudo-first order rate constant that depends on
 75 copper ion concentration ($k^I = k^I[Cu]$), D_{aq} is the HO₂ diffusion constant in the aerosol and Q
 76 accounts for aqueous-phase diffusion limitations within the aerosol. k^{II} is calculated using the
 77 following equation [25]:

$$79 \quad k^{II} = \frac{k_3 + \left(\frac{K_{eq}}{[H^+]_{aq}}\right)k_5}{\left(1 + \frac{K_{eq}}{[H^+]_{aq}}\right)^2} \quad (E2)$$

80

81 where K_{eq} , k_3 and k_5 are defined above, and $[H^+]$ is obtained from the pH within the aerosol.
 82 By inputting the rate constants in Reactions 3 and 5 to obtain k^{II} into Equation 1 using the
 83 method described by Thornton et al. ²⁵, it can be predicted that for non-viscous aqueous
 84 aerosols the HO₂ uptake coefficient would become equal to the mass accommodation at a
 85 copper concentration of 2.9×10^{-3} M. Mozurkewich et al.¹⁹ performed laboratory
 86 measurements of changes in the HO₂ signal as a function of aerosol copper ion concentration.
 87 In that study, it was found that the HO₂ uptake coefficient started to increase at a concentration
 88 of $\sim 10^{-4}$ M and reached the mass accommodation at a copper concentration of $\sim 10^{-2}$ M,
 89 suggesting that the concentration of copper ions found within tropospheric aerosols may indeed
 90 be high enough to influence HO₂ uptake. However, 20 – 90 % of submicron particulate mass
 91 is attributable to organics ^{26, 27}, and it is known that organics can act as surfactants, bind with
 92 metal ions and increase the viscosity of the aerosols ^{22, 25, 28-30}. All of these effects would be
 93 likely to cause a decrease in the HO₂ uptake coefficient, even if high copper ion concentrations
 94 were present within the aerosol. Therefore, in this work, the effect of adding organic species,
 95 which were chosen for their likelihood of strongly binding to copper ions within the aerosols,
 96 was investigated.

97

98 **Experimental**

99

100 The experimental setup used in this work is only briefly outlined below with a detailed
 101 description given in George et al.¹⁸ The experiment consisted of an aerosol flow tube coupled

102 to a sensitive Fluorescence Assay by Gas Expansion (FAGE) instrument that measured HO₂
103 indirectly. Experiments were performed by moving an injector backwards and forwards along
104 the flow tube to release HO₂ in the absence and presence of different concentrations of aerosols
105 and measuring both the HO₂ signal and the total aerosol surface area. The relative humidity
106 was controlled by mixing a flow which had passed through a bubbler with a dry flow to form
107 a humidified flow (3.0 ± 0.2 lpm), this was mixed with an aerosol flow (1.0 ± 0.2 lpm) in a
108 conditioning flow tube before entering the aerosol flow tube. The relative humidity was
109 measured using a relative humidity probe (Rotronic Hygroclip 2) after the reaction flow tube
110 and was stable within ± 3 %.

111

112 HO₂ radicals were formed by the photolysis of water vapour using a mercury lamp (L.O.T.
113 Oriel, model 6035) followed by reaction with oxygen, found in trace amounts (normally
114 specified as 20 – 30 ppm) in the nitrogen supply used, via the following reactions:

115

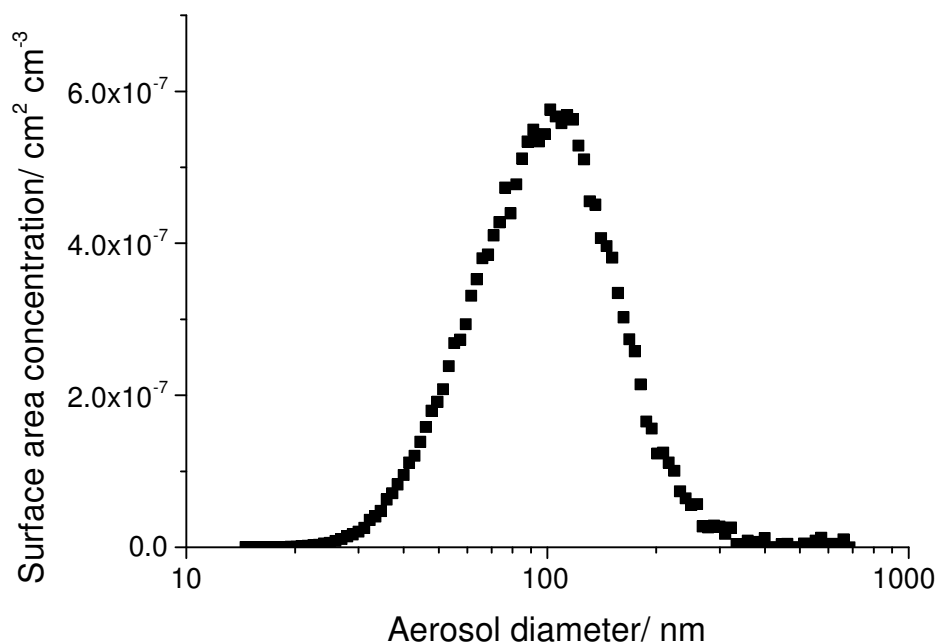


116 The HO₂ exited at the end of a moveable injector in a 1.3 ± 0.1 lpm flow where it mixed with
117 the humidified aerosol flow. HO₂ radicals were sampled at the end of the flow tube by a FAGE
118 cell which was kept at a pressure of ~ 0.85 Torr using a combination of a rotary pump (Edwards,
119 model E1M80) and a roots blower (EH1200). The HO₂ radicals were detected following their
120 conversion to OH by addition of NO, and detection of OH by laser-induced fluorescence
121 spectroscopy at 308 nm^{14, 31}. The detection limit towards HO₂, obtained by calibration, was ~
122 10⁷ molecule cm⁻³.

123

124 Atomiser solutions were prepared by dissolving 1.32 g ammonium sulphate (Fisher scientific,
125 > 99 %) and 0.125 g copper (II) sulphate pentahydrate (Fisher scientific, > 98 %) in 500 ml
126 Milli-Q water. Therefore, the molar ratio of copper ions to ammonium sulphate was one to
127 twenty and the copper molarity was estimated at a relative humidity of 60 % to be ~ 0.3 M
128 using the Aerosol Inorganic Model (AIM)^{32, 33}. Therefore, the lifetime of HO₂ within the
129 aerosol is less than one nanosecond (based upon the reaction scheme shown by Reactions 1 –

130 6), and the HO₂ uptake coefficient would therefore equal the mass accommodation coefficient.
131 Organic compounds were also added into the solution at different molar ratios to the copper
132 ions. The organics were malonic acid (Acros organics, 99 %), citric acid (Fisher scientific, >
133 99.5 %), 1,2 diaminoethane (Fisher scientific, > 98 %), tartronic acid (Sigma-Aldrich, > 97 %),
134 ethylenediaminetetraacetic acid (EDTA, Fisher scientific, 99 %) and oxalic acid (Fisher
135 scientific, > 99 %). Aerosols were formed by using an atomiser (TSI, 3076) and the
136 concentration of aerosols entering the flow tube was controlled using a high efficiency
137 particulate air (HEPA) filter and a bypass. The proportion of flow passing through the bypass
138 compared to the filter was regulated using a needle valve. Aerosols were analysed upon exiting
139 the flow tube using a Scanning Mobility Particle Sizer (SMPS, TSI, 3080) to determine the
140 overall surface area. Aerosols were passed through two neutralisers, one before the reaction
141 flow tube (Grimm 5522) and one within the SMPS (TSI 3077) giving them a known charge
142 distribution which could be accounted for by the SMPS software. An example of the size
143 distribution obtained is shown in Figure 1.



144

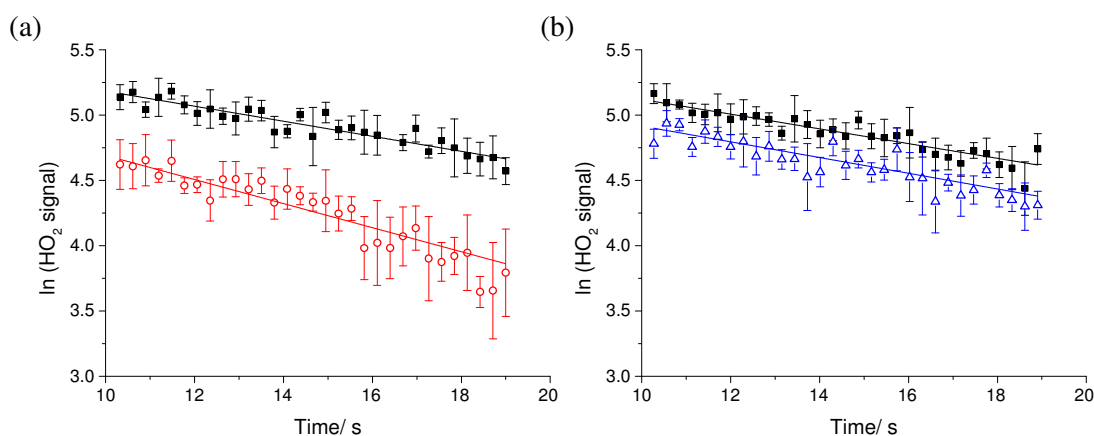
145 **Figure 1.** An example of the surface area concentration as a function of aerosol diameter for
146 copper doped ammonium sulphate aerosols containing a 2:1 oxalic acid to copper (II) ion molar
147 ratio at a relative humidity of 60 ± 3 % and at a temperature of 293 ± 2 K. The total surface
148 area concentration in this example was 1.7×10^{-5} cm² cm⁻³.

149

150 The data analysis has been previously described in detail by George et al.¹⁸ and was performed
 151 assuming pseudo-first-order kinetics, such that the HO₂ loss rate is given by the following
 152 equation:

$$\ln[HO_2]_t = \ln[HO_2]_0 - k_{obs}t \quad (E3)$$

154 where $[HO_2]_0$ is the initial concentration of HO₂, k_{obs} is the first order rate coefficient for the
 155 heterogeneous reaction of HO₂ with the aerosol particles and t is the reaction time. Examples
 156 of the background subtracted FAGE signal plotted against time in both the absence and
 157 presence of different aerosol concentrations are shown in Figure 2.



158 **Figure 2.** Pseudo-first order HO₂ temporal decays at RH = 60 ± 3 % in the absence of aerosols
 159 (black points) and with copper doped ammonium sulphate aerosols containing (a) a 2:1 oxalic
 160 acid to copper ion molar ratio at an aerosol surface area concentration of 1.7 × 10⁻⁵ cm² cm⁻³
 161 (red points), and (b) a 10:1 oxalic acid to copper ion molar ratio at an aerosol surface area
 162 concentration of 1.4 × 10⁻⁴ cm² cm⁻³ (blue points). The error bars represent one standard
 163 deviation in the measured HO₂ signal measured at each point, which is averaged for 3 seconds.
 164 The gradient of these lines were used to determine k_{obs} from Equation 3. The lower initial signal
 165 in the presence of aerosols compared to the signal in the absence of aerosols is due to
 166 measurements starting after 10 seconds reaction time.
 167

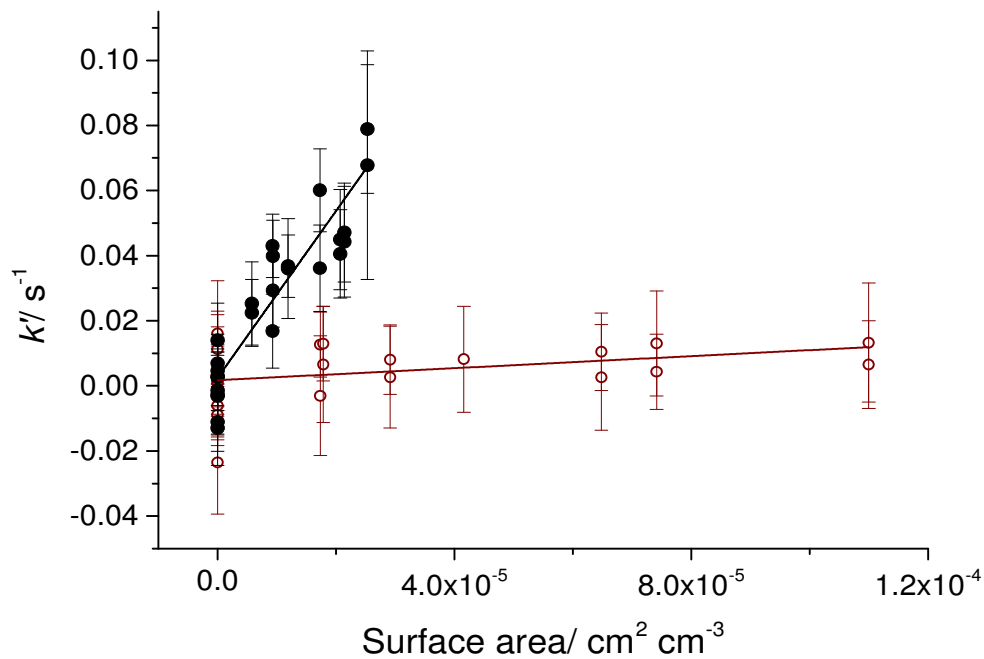
168
 169 The observed pseudo-first order rate constants were then corrected for the non-plug flow within
 170 the flow tube using the iterative procedure outlined by Brown³⁴. The Brown correction
 171 increased the pseudo-first-order rate constants on average by 34 %. The first order rate constant
 172 that had been corrected for the Brown correction (k') is related to the uptake coefficient (γ_{obs})
 173 by the following equation:

174

$$k' = \frac{\gamma_{obs}\omega_{HO_2}}{4} S \quad (E4)$$

175 where ω_{HO_2} is the molecular thermal speed of HO_2 ($cm\ s^{-1}$) and S is the total surface area of
 176 aerosols in a given volume ($cm^2\ cm^{-3}$). Therefore, k' against S was plotted for all of the
 177 experiments and an example is shown in Figure 3.

178



179

180 **Figure 3.** The pseudo-first order rate constants as a function of aerosol surface area for copper
 181 (II) doped ammonium sulfate aerosols (black) and with a 1:1 EDTA to copper molar ratio added
 182 to the aerosol. For pure copper (II) doped aerosols only a much smaller aerosol concentration
 183 range could be used as the HO_2 signal at $\sim 11 - 19$ seconds decreased to near background levels
 184 at higher aerosol concentrations.

185

186 The uptake coefficient was corrected in order to take into account gas phase diffusion. A
 187 correction for this gas phase diffusion effect was performed using the methodology described
 188 by Fuchs and Sutagin³⁵ and changed the uptake coefficient by less than 1 %.

189

190

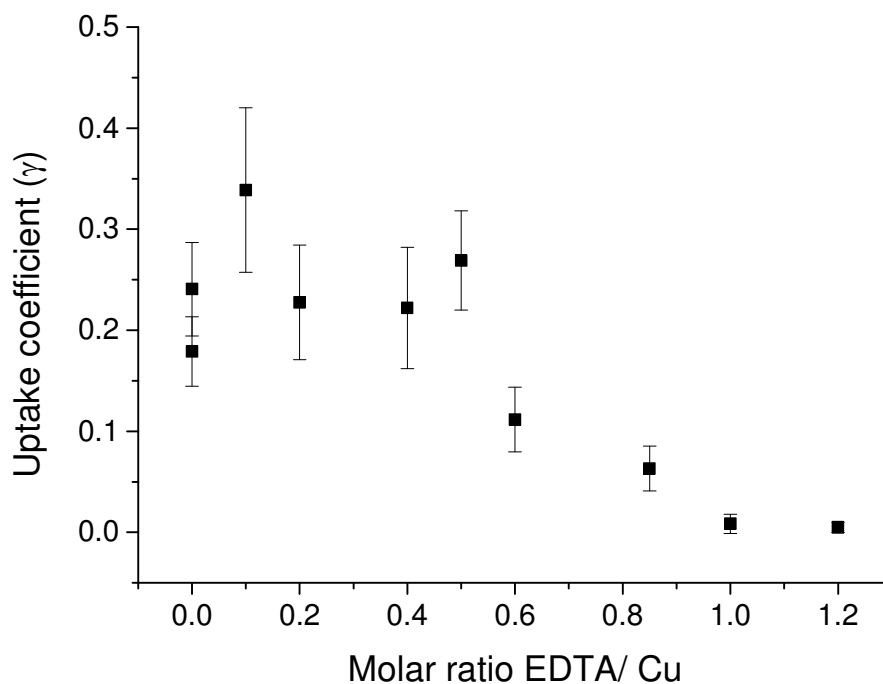
191 **Results and discussion**

192

193 The HO₂ uptake coefficient was first measured onto copper (II) sulphate doped ammonium
194 sulphate aerosols, with an example of k' plotted against aerosol surface area for this aerosol
195 type shown in Figure 3. The average HO₂ uptake coefficient was measured as 0.23 ± 0.07 over
196 the relative humidity range of 60 – 75 % and at an initial HO₂ concentration of 1×10^9 molecule
197 cm⁻³, a value that was expected to be equal to the HO₂ mass accommodation (α). The mass
198 accommodation value is in agreement (within error) of the previous measurement of $\alpha = 0.4 \pm$
199 0.3 by George et al.¹⁸ made with the same experimental setup and also agrees with the value of
200 $\alpha > 0.2$ measured by Mozurkewich et al.¹⁹ However, this value is lower than the mass
201 accommodation values of $\alpha = 0.5 \pm 0.1$ and $\alpha = 0.53 \pm 0.12$ measured by Thornton and Abbatt
202 ²¹ and Taletani et al.²⁰, respectively. Although the reason for this discrepancy remains unclear,
203 George et al.²⁰ previously showed that the HO₂ mass accommodation coefficient is larger both
204 for shorter interaction times between HO₂ and the aerosol, and for lower HO₂ concentrations.
205 Therefore, the difference in the mass accommodation between the various studies may be due
206 to varying experimental conditions, for example the longer reaction times utilised in this work
207 of ~ 10 seconds at the start of the decay to ~19 seconds at the end of the decay compared to ~
208 5 - 11 seconds used by Taketani et al.²⁰ and ~ 7 - 16 seconds used by Thornton and Abbatt.²¹

209

210 Several publications have suggested that organic species in aerosols could act as ligands for
211 transition metal ions found in tropospheric aerosols^{25, 29, 36-38}. If the organic species were acting
212 as a ligand it could cause the copper ions to be unavailable for the catalytic destruction of HO₂
213 within the aerosol as shown in Reactions 1 - 6. Therefore, in order to test this hypothesis a very
214 strongly binding hexadentate ligand (EDTA) with a binding constant of 18.8 ³⁹ towards copper
215 (II) ions was added into the copper doped ammonium sulphate aerosols in different molar ratios
216 with the copper ion. As shown in Figure 3 the gradient of k' plotted against aerosol surface area
217 reduced significantly when EDTA was added in a 1:1 molar ratio with copper. Figure 4 shows
218 that the uptake coefficient started to reduce from the mass accommodation value of 0.23 ± 0.07
219 when the molar ratio of EDTA to copper was greater than 0.5.



220

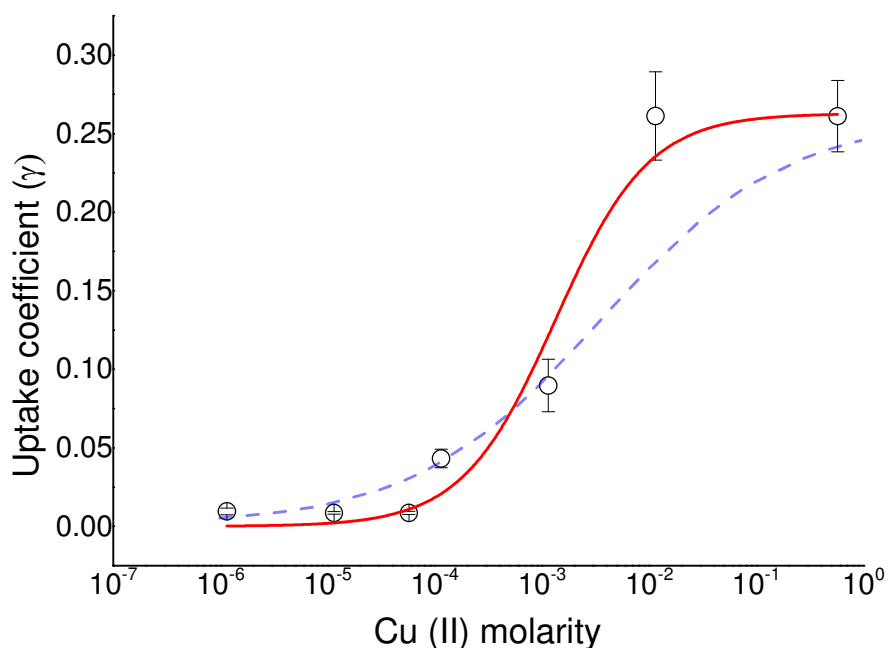
221 **Figure 4.** The HO₂ uptake coefficient for aerosols containing copper (II) doped ammonium
 222 sulphate aerosols as a function of the molar ratio of EDTA to copper in the aerosols.
 223 Experiments were performed at RH = 72 ± 4 % and at T = 293 ± 2 K. The error bars represent
 224 two standard deviations.

225

226 When the EDTA to copper (II) molar ratio was 1:1, the uptake coefficient was $\gamma = 0.009 \pm$
 227 0.009 and at an EDTA to copper molar ratio of 6:5 the uptake coefficient was $\gamma = 0.005 \pm 0.005$
 228 suggesting that the EDTA molecules binding to the copper ions make them unavailable for the
 229 catalytic destruction of HO₂ radicals.

230

231 To test whether the reduction in free (uncomplexed) Cu ion concentrations in the aerosol due
 232 to EDTA complexation with Cu alone could explain the decrease in the HO₂ uptake coefficient,
 233 HO₂ uptake coefficients were measured with aerosols containing different ammonium sulphate
 234 to copper (II) molar ratios, but in the absence of EDTA. The copper (II) concentration within
 235 the aerosols was estimated using the AIM model by assuming that both the ammonium sulphate
 236 molarity and the copper ion molarity would change by the same percentage between the
 237 atomiser solution and the aerosols. The results of this experiment are shown in Figure 5 and
 238 show that the HO₂ uptake coefficient starts to increase at an aerosol copper ion molarity of ~
 239 10^{-4} M and is fully limited by mass accommodation at an aerosol copper molarity of ~ 10^{-2} M



240

241 **Figure 5.** The HO₂ uptake coefficient as a function of the estimated Cu(II) molarity in the
 242 ammonium sulphate aerosols (estimated using the AIM model) at RH = 65 % and T = 293 ± 2
 243 K. The error bars are 2 standard deviations. The red line represents a non-linear least-squares
 244 fitting of $1/\gamma = 1/\alpha + 1/(A \times [\text{Cu}])$ to the data (Equation 5). From the fit $\alpha = 0.26$ and $A =$
 245 197 M^{-1} . The dashed blue line represents the uptake coefficient derived from Equation 1 and
 246 assuming a pH of 5 but decreasing k' by approximately 4 orders of magnitude. See text for
 247 details.

248

249 The HO₂ uptake coefficient (γ) dependence upon the copper concentration within ammonium
 250 sulphate aerosols was well described by the following equation at aerosol copper molarities >
 251 10^{-5} M :

252

$$\frac{1}{\gamma} = \frac{1}{\alpha} + \frac{1}{A[\text{Cu}]} \quad (\text{E5})$$

253 where A was determined from the best-fit to the data to be 197 M^{-1} and $\alpha = 0.26$. Equation 5 is
 254 loosely based upon the resistor model⁴⁰ with the first term being due to the mass
 255 accommodation of HO₂ and the second term due to reaction of HO₂ with Cu^{II} in the aerosol. A
 256 saturation term was not required meaning that the reaction was fast and would occur near the
 257 surface of the aerosol. The HO₂ uptake coefficient dependence upon aerosol copper molarities
 258 measured in this work is in agreement with the measurements made by Mozurkewich et al.¹⁹,

259 who observed a changing HO₂ signal with a similar functional form with aerosol copper
260 molarity. However, the measured dependence does not necessarily agree with the rate constants
261 for the known aqueous chemistry shown in Reactions 1 – 6, as discussed previously by
262 Thornton et al.²⁵. If the literature rate constants for Reactions 1 - 6 are entered into Equation 1,
263 using the methodology described by Thornton et al.²⁵, it would be expected that the HO₂ uptake
264 coefficient would be fully limited by the mass accommodation at a copper molarity of $\sim 10^{-4}$
265 M, rather than the experimental value of $\sim 10^{-2}$ M. The dashed blue line in Figure 5 shows the
266 best fit that could be obtained to the data using Equation 1. However, in order to achieve this
267 best-fit, the product $k^I = k^{II}[\text{Cu}]$ had to be reduced by approximately 4 orders of magnitude,
268 requiring a reduction in the copper ion concentration and/or the rate constants R3 and R5 used
269 to determine k^I as given by Equation 2.

270

271 There are several factors that may account for such a large change being required in order to
272 fit Equation 1 to the data in Figure 5. On the one hand, the Cu^{II} concentrations in the aerosols
273 have been calculated by a model that has not been specifically developed for Cu^{II}. It has been
274 assumed that copper sulphate behaves like ammonium sulphate, which may introduce large
275 errors in concentration determination. On the other hand, for a supersaturated
276 microenvironment like aerosols, it may be more appropriate to use activities instead of
277 concentrations in Equation 1, owing to the strong ionic interactions that are present. However,
278 for a similar type of aerosol, Mao et al.²³ calculated that the Cu reactivity could decrease at
279 most by about 1 order of magnitude owing to a reduction of its activity, meaning that a
280 significant change in k^I is still needed in order to adequately fit the data in Figure 5.

281

282 Moreover, the reduction in reactivity is likely to be due, at least in part, to the
283 microenvironment of the copper ions within the aerosols where the concentration of ‘free’
284 copper and/or the reactivity of copper could decrease. Following uptake of HO₂ radicals and
285 diffusion, the reactions occur within supersaturated aerosols containing relatively high
286 concentrations of dissolved ions. In contrast, the rate constants used in the calculations to obtain
287 k^{II} were measured from kinetics experiments undertaken in more dilute solutions. Using Raman
288 spectroscopy and an electrodynamic balance, Zhang et al.⁴¹ found that at high concentrations,
289 chemical interactions between sulfate ions with the metallic counter-cations were significant
290 and led to the formation of contact ion pairs that modified the hygroscopic properties of the

291 aerosol. Zhang et al.⁴¹ showed that contact ion pair mixtures shared sulphate ions and water
292 molecules and those empirical mixing rules of water activity of atmospheric aerosols became
293 invalid. Such effects and changes in molecular structures in a concentrated aerosol may reduce
294 the reactivity or availability of Cu ions and hence k^I and explain, in part, why a significant
295 reduction to the rate constants is required. In addition, Zhang et al.⁴¹ also state that similar
296 effects may occur in metal-organic ion systems.

297

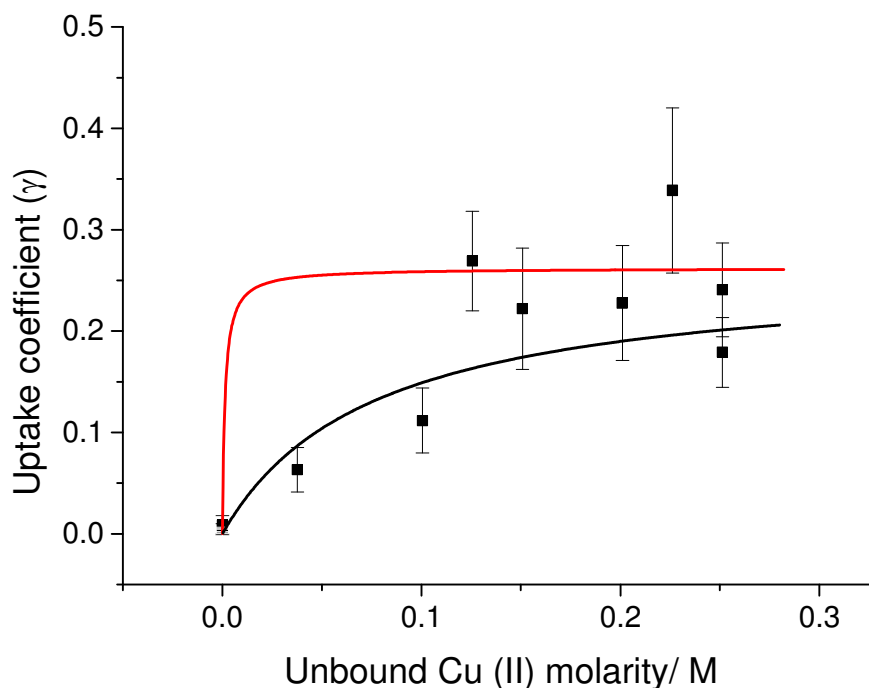
298 Finally, there are other parameters which would influence the right-hand term of Equation 1
299 which controls the functional form of the Thornton et al. (2008) expression for the uptake
300 coefficient versus copper molarity. We have already considered changes to k_3 , k_5 , [Cu] and
301 above. The value of α^{HO_2} , used in the first term of Equation 1 is constrained to the measured
302 value and only impacts the value at high [Cu]. Assuming w , the molecular thermal speed of
303 HO₂, R and T are accurate, then this leaves H_{eff} , the Henry's laws constant, D_{aq} the HO₂
304 diffusion constant in the aerosol and Q , which allows for aqueous-phase diffusion limitations
305 within the aerosol. Also, in order to calculate k^{II} , the values of K_{eq} and $[\text{H}^+]$ are required. H_{eff}
306 could be reduced owing to the microenvironment, although the mechanism for this is unclear
307 (we discuss H_{eff} further below when organic-complexation can occur). D_{aq} for HO₂ has not
308 been measured directly in aerosols themselves and so would be subject to uncertainty. As the
309 aerosols are aqueous, diffusion limitations would not be expected, and so Q is likely to be very
310 close to 1 (this may not be true for more viscous aerosols such as secondary organic aerosols).
311 K_{eq} is very well established, but there is some uncertainty in the pH of the aerosol. 0.1 M – 2 M
312 ammonium sulfate (a weak acid) solutions have a pH of between 5.5 and 6, and as the copper
313 sulfate is also a weak acid and could also slightly acidify the aerosol (although being present
314 at a much lower concentration), a pH of 5 was estimated for the aerosol and used in Equation
315 1. However, the true pH is unknown and may be considerably different to the pH 5 used.

316

317 In summary, there are several parameters in Equation 1 which have significant uncertainties,
318 and when acting together could account for the four orders of magnitude change that are needed
319 compared to the values in Thornton et al. (2008) to adequately fit the data shown in Figure 5.

320

321 Figure 6 shows the measured HO₂ uptake coefficients in the presence of EDTA as a function
 322 of free copper ions, and also a comparison with the HO₂ uptake coefficients calculated using
 323 Equation 5, using the best parameterised fit ($A=197 \text{ M}^{-1}$) to the data shown in Figure 5.



324
 325 **Figure 6.** The HO₂ uptake coefficient for aerosols containing copper doped ammonium
 326 sulphate aerosols as a function of the concentration of the unbound Cu (II) ions assuming that
 327 EDTA binds to copper in a one to one ratio. The red line ($R^2 = 0.72$) represents the expected
 328 change in uptake coefficient controlled only by the changing copper (II) concentrations as
 329 given by Equation 5, and the black line ($R^2 = 0.89$) is the best fit of Equation 6 to the data,
 330 which assumes that an additional process is also controlling the change in the HO₂ uptake
 331 coefficient. Experiments were performed at $RH = 72 \pm 4 \%$ and $T = 293 \pm 2 \text{ K}$. The error bars
 332 represent two standard deviations of the propagated error in the gradient of the k' against
 333 surface area graphs. See text for details.

334
 335 It can be seen that the measured HO₂ uptake coefficient in the presence of EDTA increases
 336 considerably more slowly with [Cu(II)] compared with the uncomplexed case. Figures 5 and 6
 337 can be directly compared due to the similar conditions under which these experiments were
 338 performed. A one-to-one binding ratio of copper ions to EDTA has been used to estimate the
 339 free copper ion molarity within the aerosols. For copper ion concentrations below 0.1 M the
 340 measured HO₂ uptake coefficients tend to fall below the calculated value from Equation 5,
 341 suggesting that the HO₂ uptake coefficient is not purely controlled by the binding of EDTA to
 342 the copper ions, which would make it unavailable for catalytic destruction of HO₂. A better fit

343 ($R^2 = 0.89$ versus 0.72) to the measurements was obtained using a modified form of Equation
 344 5, which is also shown in Figure 6:

345

$$\frac{1}{\gamma} = \frac{1}{\alpha} + \frac{1}{197[Cu(II)]} + \frac{1}{B[Cu(II)]} \quad (E6)$$

346

347 where the parameter B , which reduces the uptake coefficient potentially as a result of the EDTA
 348 acting as a surfactant or causing a change in the viscosity of the aerosols, was found to be 3.5
 349 M^{-1} . It has previously been shown that surfactants can reduce the uptake coefficient of a species
 350 by either forming a diffusion barrier, thereby reducing the mass accommodation coefficient, or
 351 by decreasing the Henry's law coefficient⁴¹⁻⁴³. If EDTA was causing a change of viscosity
 352 within the aerosol it would also be expected that the HO_2 uptake coefficient would decrease
 353 due to slower diffusion of HO_2 into the bulk of the aerosol. The impact of viscosity upon uptake
 354 coefficients has previously been shown to be important and has been investigated on other
 355 systems such as the ozonolysis of oleic acid and the rate of heterogeneous reaction of particle-
 356 borne benzo[a]pyrene (BaP) with ozone within SOA particles^{44, 45}. However, it is currently not
 357 possible to state with certainty which of these effects EDTA had upon the aerosol properties
 358 that caused the HO_2 uptake coefficient to decrease at a faster rate than expected when the EDTA
 359 concentrations within the aerosols were increased. More fundamental experiments would be
 360 required such as measuring the surface tension of the aerosols or measuring the diffusion of
 361 species through the aerosols in the presence and absence of EDTA. We return to the discussion
 362 regarding changes in viscosity or surface coatings after presenting the results for HO_2 uptake
 363 coefficients in the presence of other organic species.

364

365 However, as EDTA is not observed within tropospheric aerosols, other organic species were
 366 also investigated to determine whether these would similarly reduce the HO_2 uptake coefficient
 367 onto copper doped aerosols. Experiments were performed with malonic acid, citric acid, 1,2
 368 diaminoethane, tartronic acid and oxalic acid. These species were chosen because of their
 369 likelihood to bind with metals in the aerosol based upon their Henry's law constant and their
 370 binding constant with copper (II) ions, and because of their presence in the atmosphere²⁹. It
 371 should be noted that Okochi and Brimblecombe²⁹ predicted that based upon the Henry's law
 372 constant and their binding constants with copper (II), similar molarities (within 20 %) of oxalic

373 acid and tartronic acid would bind to a given copper (II) concentration, whereas the molarity
 374 of malonic acid would have to be at least an order of magnitude larger for it to bind to the same
 375 copper concentration.

376

377 Experiments were performed with either a 2:1 or a 10:1 organic to copper molar ratio within
 378 the atomiser solution and the relationships between the pseudo-first order rate constants and
 379 the aerosol surface areas are shown in Figure 7 and summarised in Table 1. However, it should
 380 be noted that for volatile organics the ratios may decrease within the aerosols.

381

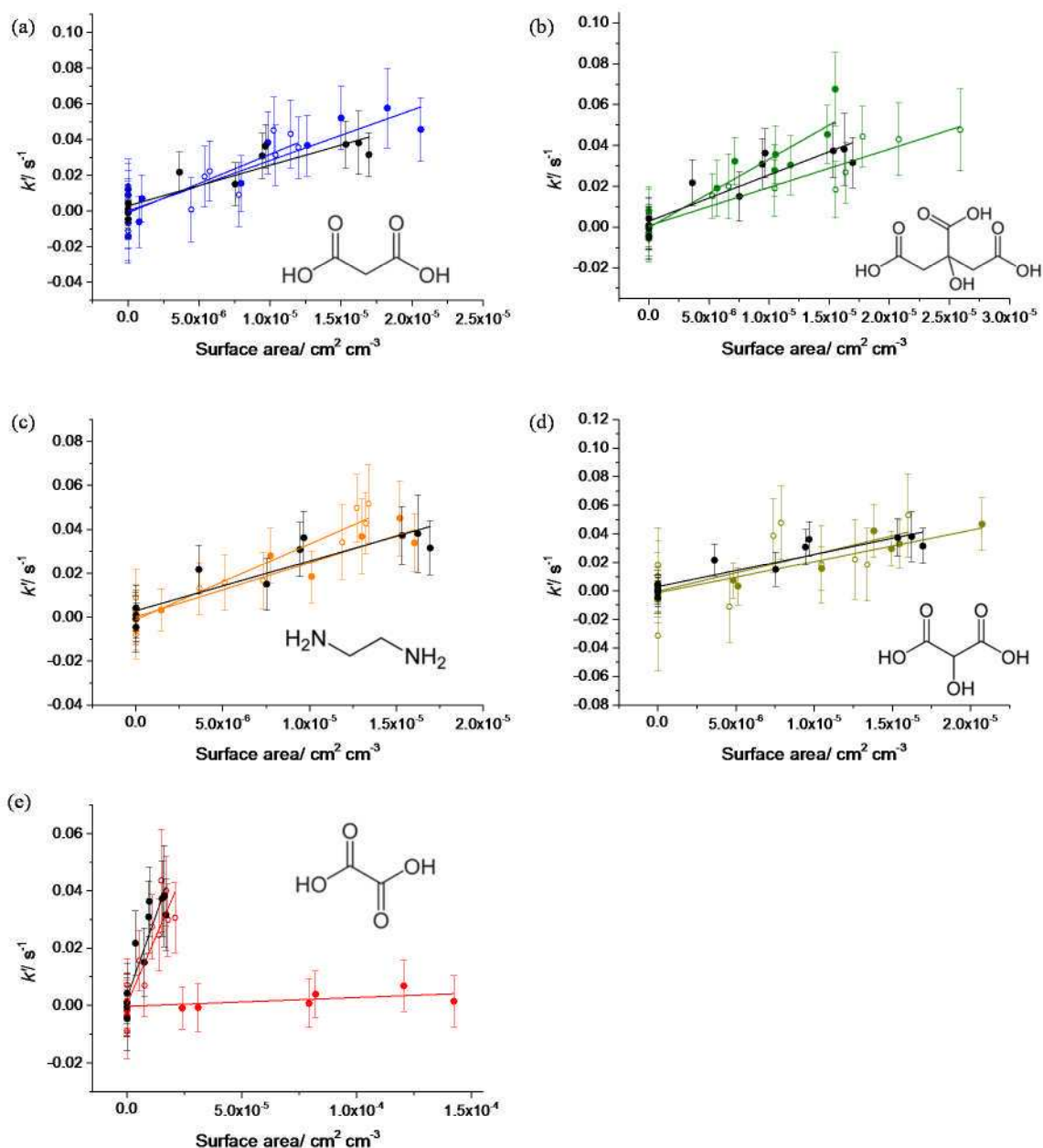
Organic	HO ₂ uptake coefficient for a given organic : copper sulphate molar ratio	
	2:1	10:1
Malonic acid	0.32 ± 0.09	0.28 ± 0.06
Citric acid	0.17 ± 0.05	0.31 ± 0.08
1,2 diaminoethane	0.32 ± 0.07	0.24 ± 0.05
Tartronic acid	0.24 ± 0.15	0.19 ± 0.07
Oxalic acid	0.17 ± 0.05	0.003 ± 0.004

382

383

384 **Table 1.** Uptake coefficients measured for copper (II) sulphate doped ammonium aerosols
 385 containing either a 2:1 or a 10:1 organic to copper (II) molar ratio. All experiments were
 386 performed at RH = 60 ± 3 % and T = 293 ± 2 K, and the estimated copper molarity within all
 387 of the aerosols was ~ 0.3 M. The error bars represent two standard deviations of the propagated
 388 error in gradients of the graphs of the pseudo-first order rate constant k' against aerosol surface
 389 area, S . The mass accommodation value obtained when no organics were present in the aerosols
 390 was $\alpha = 0.23 \pm 0.07$.

391



392

393 **Figure 7.** The pseudo-first order rate constants as a function of aerosol surface area for copper
 394 (II) doped ammonium sulfate aerosols (black, shown in all panels) and with (a) malonic acid
 395 (blue), (b) citric acid (green), (c) 1,2 diaminoethane (orange), (d) tartronic acid (dark yellow)
 396 and (e) oxalic acid (red) added. The open coloured symbols represent a 2:1 molar ratio of the
 397 organic to the copper and the closed coloured symbols represent a 10:1 molar ratio of the
 398 organic to the copper. All experiments were performed at $RH = 60 \pm 3 \%$ and $T = 293 \pm 2 \text{ K}$.
 399 The error bars represent one standard deviation.

400

401 As shown in Table 1, when the organic species were present in the aerosols the HO₂ uptake
 402 coefficient was within error of the mass accommodation coefficient ($\alpha = 0.23 \pm 0.07$) with the
 403 exception of when oxalic acid was added into the aerosols in a 10:1 molar ratio with the copper.

404 Despite their similar chelating strengths, the difference in the effect of the addition of oxalic
405 acid and tartronic acid on the HO₂ uptake suggests that the decrease in the HO₂ uptake
406 coefficient in the presence of oxalic acid could not be purely due to copper-oxalate complexes
407 forming. The presence of oxalic acid and/ or oxalate metal complexes must have either changed
408 the properties of the aerosol (e.g. the viscosity) or the total concentration of copper within the
409 aerosols (e.g. due to precipitation).

410

411 A recent study by Drozd et al. has shown that the addition of oxalic acid to aerosols containing
412 inorganic salts (e.g CaCl₂, MgCl₂ and ZnCl₂) reduced both the volatility of the oxalic acid and
413 the hygroscopicity of the aerosol⁴⁶. The low hygroscopicities of the aerosols could either be due
414 to a large increase in the viscosity of the aerosol or the formation of a strongly-bound insoluble
415 metal-oxalate complexes (salts) forming a coating at the surface of the aerosol. An increase in
416 the aerosol viscosity from the formation of the metal-complexes may have reduced the HO₂
417 uptake coefficient due to the slow diffusion of HO₂ in the aerosol. Alternatively, formation of
418 a metal-oxalate complex precipitate in the aerosol may also have reduced the HO₂ uptake
419 coefficient with increasing oxalic acid concentrations due to lower copper concentrations
420 within the aerosol. A coating could potentially also have formed a diffusion barrier or affected
421 the HO₂ Henry's law coefficient into the aerosols as shown by previous work⁴¹⁻⁴³. However,
422 other factors that may have decreased the HO₂ uptake coefficient cannot be ruled out. For
423 example, Reactions 4 and 6 are dependent on the liquid water concentrations within the
424 aerosols that would be expected to be lower when oxalate is present within the aerosol due to
425 the lower hygroscopicity of the aerosol. However, the exact concentration of liquid water
426 within the aerosols during the HO₂ experiments onto aerosols containing copper (II) ions and
427 oxalic acid is unknown. Further experiments, such as measuring the surface tension or diffusion
428 of species through aerosols in the presence and absence of oxalate may elucidate which
429 mechanism is operating, or whether it is a combination of effects that decreases the HO₂ uptake
430 coefficient in the presence of oxalate.

431

432 Organic-inorganic component interactions are typically not considered in atmospheric models,
433 but as discussed by Drozd et al.⁴⁷ can greatly affect aerosol volatility and hygroscopicity. For
434 example, Drozd et al.⁴⁷ reported a dramatic increase in the CCN (cloud condensation nuclei)
435 activation diameter, up to 50 nm, for relatively small particle mass fractions of oxalic acid (10–
436 20 %). In particular this was found for bi-dentate binding of di-carboxylic to soluble inorganic

437 ions, being particularly strong for di-valent metal ions (e.g. Ca^{2+} , Mg^{2+} and Zn^{2+}). Surface
438 enrichment of insoluble metal-organic complexes (salts), giving a hard, insoluble coating
439 which could result in particles that are hard enough to exhibit bounce on particle impactors and
440 which could affect uptake onto those particles. Such a mechanism could operate for Cu(II) here
441 in the presence of oxalate impacting the uptake coefficient for HO_2 . The value of the effective
442 Henry's law constant for HO_2 in the aerosols would be reduced, which as a denominator term
443 in Equation 1, would result in a higher [Cu] needed to achieve a given uptake coefficient.
444

445 **Atmospheric Implications**

446
447 Dicarboxylic acids contribute ~15% of the total marine organic aerosol mass with oxalic acid
448 contributing more than 50% of the total dicarboxylic acids ⁴⁷⁻⁴⁹. During the Reactive
449 Halogens in the Marine Boundary Layer (RHAMBLE) field campaign, which took place in
450 Cape Verde, oxalate was measured as 78 – 151 ng m^{-3} in PM_{10} aerosols ⁵⁰. In this work, a 10:1
451 oxalic acid to copper molar ratio decreased the uptake coefficient by approximately three orders
452 of magnitude. Therefore, if copper was the only metal ion that could bind with oxalate, a copper
453 concentration in Cape Verde of 5.6 – 10.9 ng m^{-3} or less would be unable to catalytically
454 destroy HO_2 . The inability of the copper to catalytically destroy HO_2 would be likely to be due
455 to the precipitation of copper-oxalate complexes or an increase in the aerosol viscosity.
456 However, it should be noted that although the actual concentration of copper ions within the
457 aerosols during the RHAMBLE field campaign remains unknown, Fomba, et al. ⁵¹ recently
458 measured the copper concentration in Cape Verde as being in the range of 0.03 – 1.17 ng m^{-3} .
459 In Cape Verde there were also other metals such as iron ions that could also potentially bind
460 with oxalate and were measured in the range of 0.1 – 25.89 ng m^{-3} ⁵¹. Therefore, further
461 laboratory studies with different salts, metals, aerosol pHs, and oxalic acid to metal ratios
462 would be required in order to definitively determine the effect of oxalate in aerosols and to
463 relate this to tropospheric aerosols.
464

465 A box model which was constrained with gas-phase data taken during the RHAMBLE project
466 ⁵² that took place in 2007 at the Cape Verde Atmospheric Observatory (CVAO) ⁵³, which is
467 situated on the island of Sao Vicente in the tropical Atlantic ocean (23.96° S, 46.39° W) was
468 utilised to investigate the effect of the presence of oxalate within the aerosols during the
469 RHAMBLE field campaign. The model, which utilises the Master Chemical Mechanism v3.2,

470 has been described previously and has formerly been used to calculate OH and HO₂
471 concentrations for comparison with those measured at CVAO (Whalley et al., 2010). The effect
472 of mineral dust aerosols on HO₂ concentrations was also studied using this model^{15, 54}. As
473 stated in the Introduction, a typical copper ion concentration of 3.1 ng m⁻³ could lead to copper
474 ion concentrations of $\sim 2.9 \times 10^{-3}$ M in aerosols in rural areas, which may be high enough for
475 the HO₂ uptake coefficient to equal the HO₂ mass accommodation ($\alpha = 0.23 \pm 0.07$ in this
476 work). However, based upon the measurements made by Fomba et al.⁵¹, the copper molarity
477 within the aerosols would be unlikely to be as elevated as this. With large concentrations of
478 oxalate within the aerosols, as measured by Mueller et al.⁵⁰, the uptake coefficient would be
479 reduced ($\gamma = 0.003 \pm 0.004$ in this work, Figure 7e). Therefore, these two uptake coefficients
480 were inputted into the box model to determine the potential maximum impact upon gaseous
481 HO₂ concentrations. For $\gamma = 0.003$ and 0.23 the HO₂ gaseous concentration decreased by 0.2
482 and 15 %, respectively, at solar noon.

483

484 In this work it has been shown that oxalate ions within aerosols, and potentially other organic
485 species, may cause a significant change in the HO₂ uptake coefficient, and therefore, in the
486 gaseous HO₂ concentrations within the troposphere if the aerosols contain substantial copper
487 concentrations ($> 10^{-4}$ M).

488

489 **Conclusions**

490

491 The addition of EDTA and oxalic acid to copper (II) doped ammonium sulphate aerosols
492 decreased the HO₂ uptake coefficient significantly. For copper (II) doped ammonium sulphate
493 aerosols a HO₂ uptake coefficient (or a mass accommodation value) of 0.23 ± 0.07 was
494 measured which decreased to a value of 0.009 ± 0.009 when EDTA was added in a 1:1 molar
495 ratio with the copper (II). The HO₂ uptake coefficient decreased from 0.23 ± 0.07 to a value of
496 0.003 ± 0.004 when a ten to one oxalic acid to copper molar ratio was present in the atomiser
497 solution. However, no significant change was observed when malonic acid, citric acid or 1,2
498 diaminoethane were added to the atomiser solutions in a 10:1 molar ratio with the copper. It is
499 postulated that the decrease in the HO₂ uptake coefficient from the presence of EDTA in the
500 aerosols was due in part to EDTA binding to the copper (II) ions, reducing the free copper (II)
501 concentration and making it unavailable to catalytically destroy the HO₂. Experiments

502 performed in the absence of any added organic species was used to measure the variation of γ
503 as a function of concentration of the free copper (II). The uptake coefficient increased from a
504 very low value towards the mass accommodation coefficient at a much higher concentration of
505 Cu(II) than expected by the expression developed by Thornton et al.²⁵ using available kinetic
506 data. This finding provides evidence that in the supersaturated ammonium sulphate aerosols
507 contact ion pairs or complex structures are present which significantly reduces the reactivity of
508 copper ions towards HO₂. There may also be uncertainties in the pH within the aerosol used to
509 calculate the uptake coefficient.

510

511 In the presence of EDTA, the HO₂ uptake coefficient as a function of the free copper ion
512 concentration calculated assuming a 1:1 complex was significantly different to that obtained in
513 the absence of EDTA, suggesting that γ is not purely controlled by the binding of EDTA to the
514 copper ions. EDTA may have acted as a surfactant or changed the viscosity of the aerosol,
515 which would have reduced the diffusion coefficient of HO₂ within the aerosol resulting in a
516 reduction in γ . It is hypothesized that the decrease in the HO₂ uptake coefficient when oxalic
517 acid was added to the aerosols was due to either formation of a strongly-bound Cu-oxalate salt
518 which is not soluble, forming a surface coating (preventing HO₂ reaching the bulk of the
519 aerosol) or a precipitate which reduces further the concentration of free copper ions, or (b) there
520 is a reduction in the bulk viscosity of the aerosol caused by the formation of strongly-bound
521 metal-organic complexes, and hence reducing the diffusion constant of HO₂.

522

523 Overall, it has been shown that organic species within aerosols have the potential to decrease
524 the HO₂ uptake coefficient significantly (from $\gamma = \alpha$ if there are sufficient transition metal ions
525 within the aerosol), and thereby can have a significant impact on gaseous HO₂ concentrations
526 within the troposphere. Although it is important to know the transition metal ion concentration
527 within aerosols when predicting the HO₂ uptake coefficient, it is also extremely important to
528 measure the organic content of the aerosol and to identify species that could affect the
529 properties of the aerosol by binding to metals within the aerosol, by changing the viscosity of
530 the aerosol or by acting as surfactants at the surface of the aerosol. However, in order to better
531 understand the effect that organic species have upon the properties of the aerosol, and therefore
532 on gaseous tropospheric HO₂ concentrations, more laboratory measurements are needed at
533 different relative humidities, with different organic species at different concentrations and with

534 mixtures of transition metal ions within the aerosols. Experiments to measure the surface
535 tension of the aerosols and measuring the diffusion of species through the aerosols in the
536 presence and absence of organics is also highly desirable, in order to understand the mechanism
537 by which these organics change the value of the HO₂ uptake coefficient.

538

539 **Acknowledgements**

540

541 This work was supported by the National Environment Research Council under grant
542 NE/F020651/1. PSJL is grateful to NERC for the award of a studentship. LKW and DEH are
543 also grateful to the National Centre for Atmospheric Science, which is funded by NERC, for
544 ongoing support.

545

546 **Tables**

547 **Table 1.** Uptake coefficients measured for copper (II) sulphate doped ammonium aerosols
 548 containing either a 2:1 or a 10:1 organic to copper (II) molar ratio. All experiments were
 549 performed at $RH = 60 \pm 3 \%$ and $T = 293 \pm 2 \text{ K}$, and the estimated copper molarity within all
 550 of the aerosols was $\sim 0.3 \text{ M}$. The error bars represent two standard deviations of the propagated
 551 error in gradients of the graphs of the pseudo-first order rate constant k' against aerosol surface
 552 area, S . The mass accommodation value obtained when no organics were present in the aerosols
 553 was $\alpha = 0.23 \pm 0.07$.

554

Organic	HO_2 uptake coefficient for a given organic : copper sulphate molar ratio	
	2:1	10:1
Malonic acid	0.32 ± 0.09	0.28 ± 0.06
Citric acid	0.17 ± 0.05	0.31 ± 0.08
1,2 diaminoethane	0.32 ± 0.07	0.24 ± 0.05
Tartronic acid	0.24 ± 0.15	0.19 ± 0.07
Oxalic acid	0.17 ± 0.05	0.003 ± 0.004

555

556

557

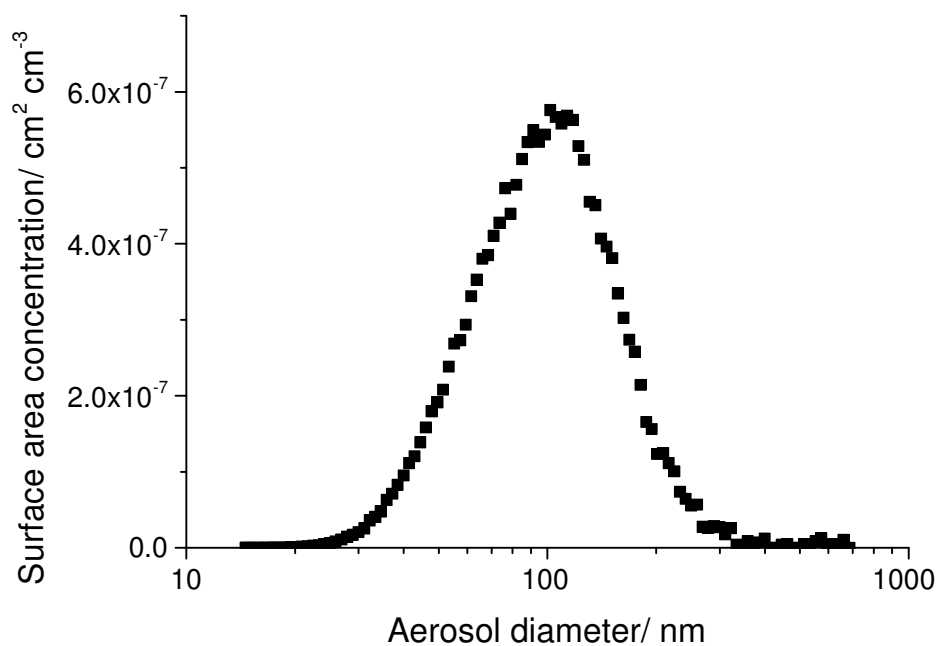
558 **Figures**

559

560

561

562



563

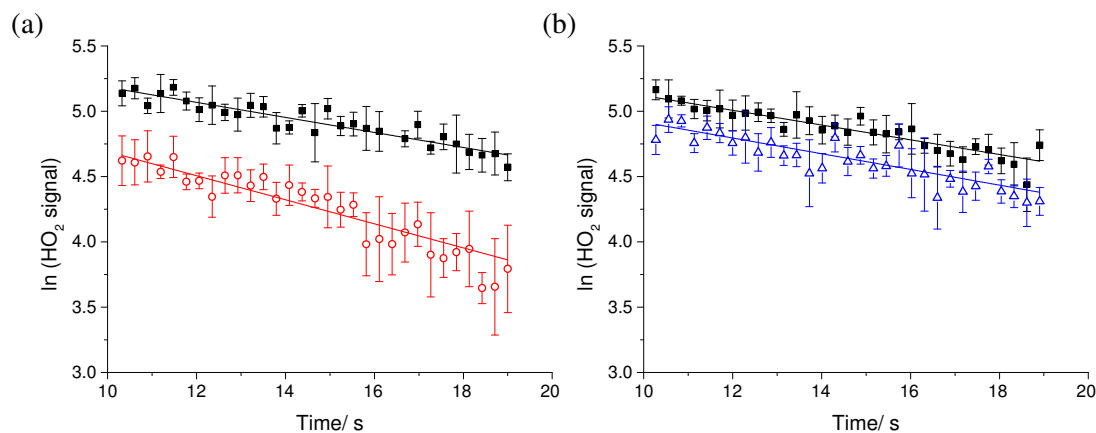
564

565 **Figure 1.** An example of the surface area concentration as a function of aerosol diameter for
566 copper doped ammonium sulphate aerosols containing a 2:1 oxalic acid to copper (II) ion molar
567 ratio at a relative humidity of 60 ± 3 % and at a temperature of 293 ± 2 K. The total surface
568 area concentration in this example was 1.7×10^{-5} cm² cm⁻³.

569

570

571



572

573 **Figure 2.** Pseudo-first order HO₂ temporal decays at RH = 60 ± 3 % in the absence of aerosols
 574 (black points) and with copper doped ammonium sulphate aerosols containing (a) a 2:1 oxalic
 575 acid to copper ion molar ratio at an aerosol surface area concentration of 1.7 × 10⁻⁵ cm² cm⁻³
 576 (red points), and (b) a 10:1 oxalic acid to copper ion molar ratio at an aerosol surface area
 577 concentration of 1.4 × 10⁻⁴ cm² cm⁻³ (blue points). The error bars represent one standard
 578 deviation in the measured HO₂ signal measured at each point, which is averaged for 3 seconds.
 579 The gradient of these lines were used to determine *k_{obs}* from Equation 2. The lower initial signal
 580 in the presence of aerosols compared to the signal in the absence of aerosols is due to
 581 measurements starting after 10 seconds reaction time.

582

583

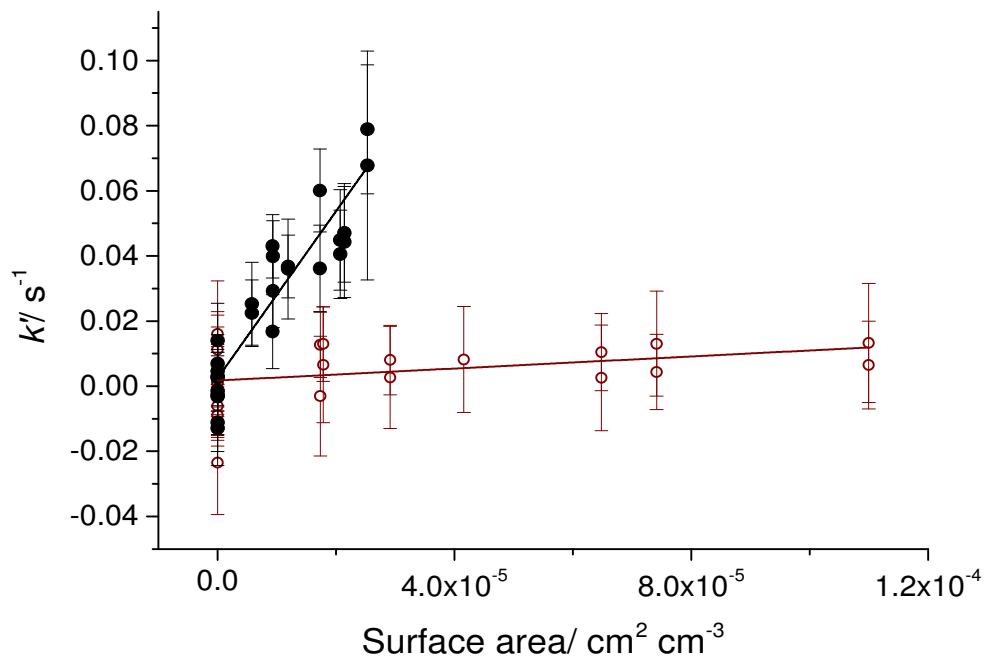
584

585

586

587

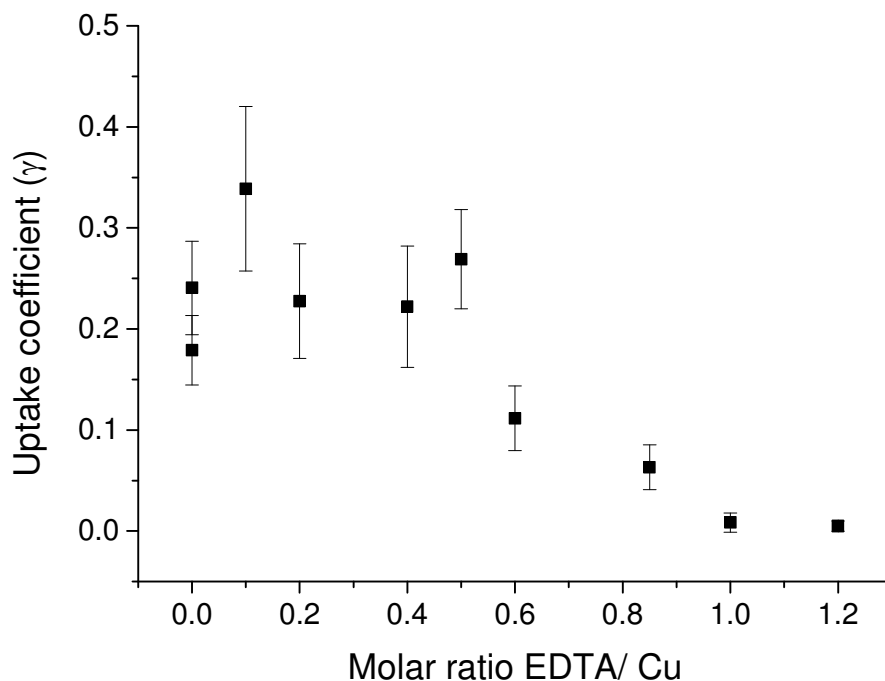
588



589

590 **Figure 3.** The pseudo-first order rate constants as a function of aerosol surface area for copper
591 (II) doped ammonium sulfate aerosols (black) and with a 1:1 EDTA to copper molar ratio added
592 to the aerosol. For pure copper (II) doped aerosols only a much smaller aerosol concentration
593 range could be used as the HO_2 signal at $\sim 11 - 19$ seconds decreased to near background levels
594 at higher aerosol concentrations.
595

596



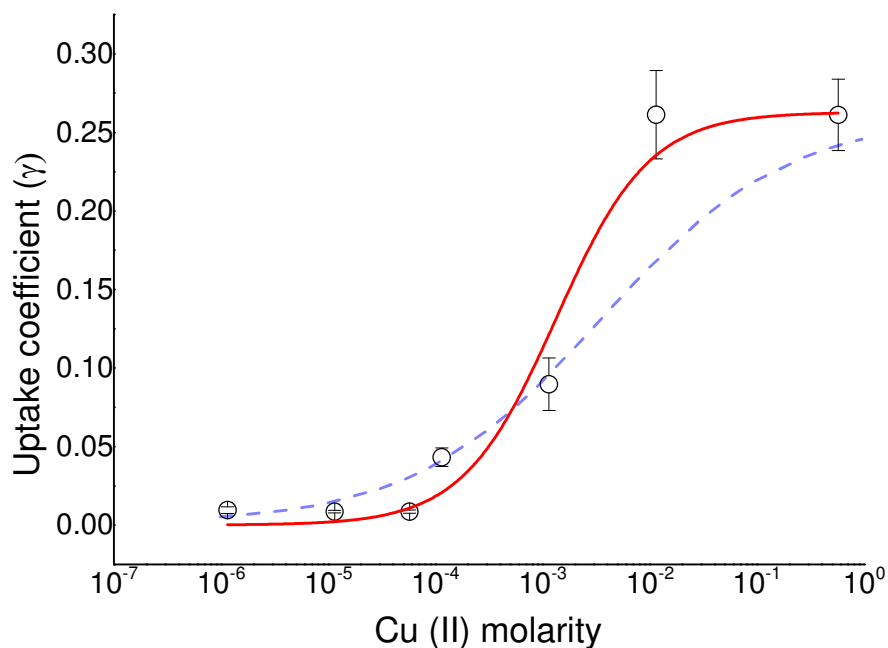
597

598 **Figure 4.** The HO₂ uptake coefficient for aerosols containing copper (II) doped ammonium
599 sulphate aerosols as a function of the molar ratio of EDTA to copper in the aerosols.
600 Experiments were performed at RH = 72 ± 4 % and at T = 293 ± 2 K. The error bars represent
601 two standard deviations.

602

603

604



605

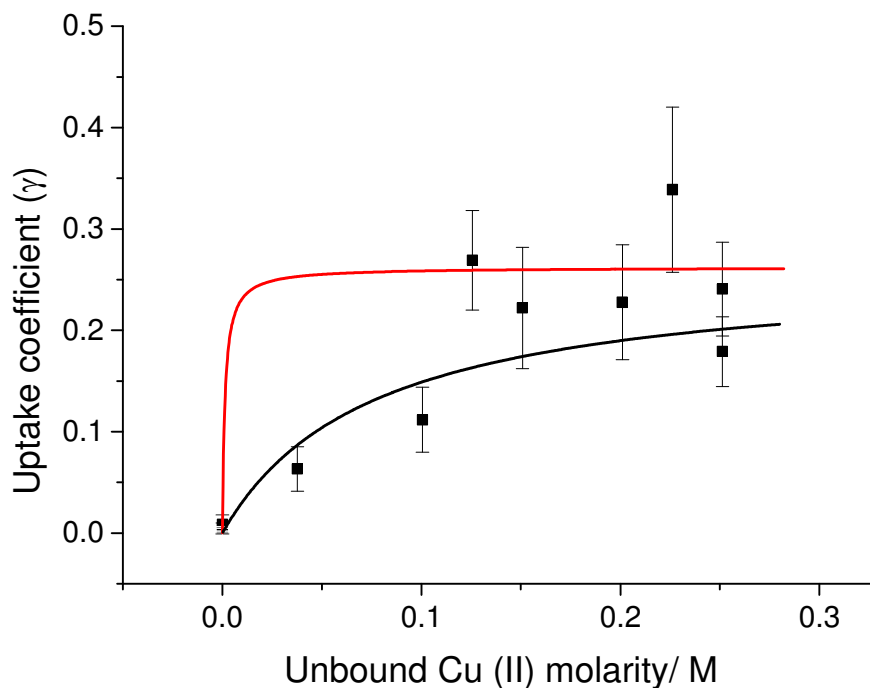
606 **Figure 5.** The HO₂ uptake coefficient as a function of the estimated Cu(II) molarity in the
 607 ammonium sulphate aerosols (estimated using the AIM model) at RH = 65 % and T = 293 ± 2
 608 K. The error bars are 2 standard deviations. The red line represents a non-linear least-squares
 609 fitting of $1/\gamma = 1/\alpha + 1/(A \times [\text{Cu}])$ to the data (Equation 5). From the fit $\alpha = 0.26$ and $A =$
 610 197 M^{-1} . The dashed blue line represents the uptake coefficient derived from Equation 1 and
 611 assuming a pH of 5 but decreasing k' by approximately 4 orders of magnitude. (either due to a
 612 reduction of the rate constants for R3 and R5 or in the copper ion concentration, or a
 613 combination of both). See text for details.

614

615

616

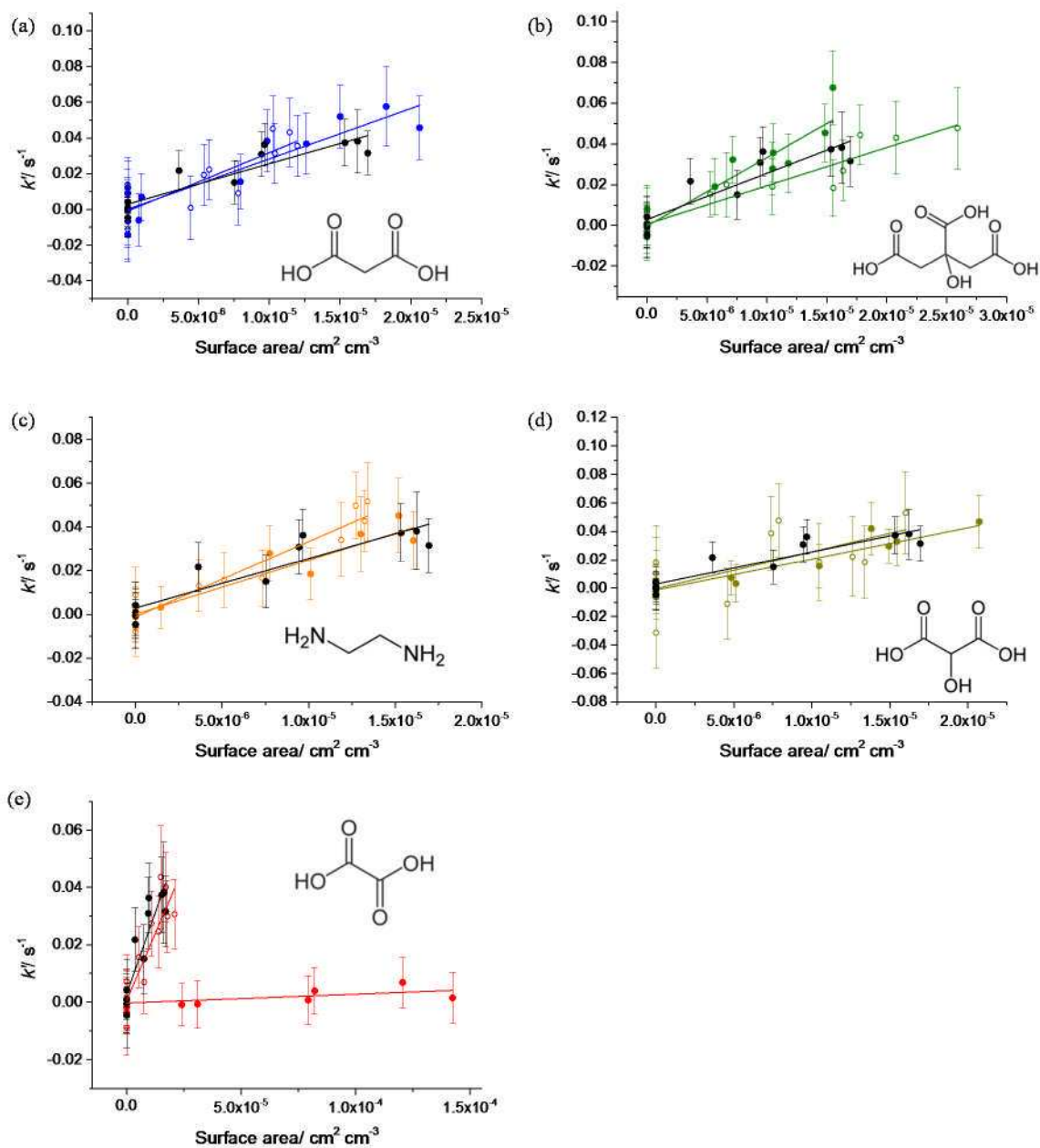
617



618

619 **Figure 6.** The HO₂ uptake coefficient for aerosols containing copper doped ammonium
 620 sulphate aerosols as a function of the concentration of the unbound Cu (II) ions assuming that
 621 EDTA binds to copper in a one to one ratio. The red line ($R^2 = 0.72$) represents the expected
 622 change in uptake coefficient controlled only by the changing copper (II) concentrations as
 623 given by Equation 5, and the black line ($R^2 = 0.89$) is the best fit of Equation 6 to the data,
 624 which assumes that an additional process is also controlling the change in the HO₂ uptake
 625 coefficient. Experiments were performed at $RH = 72 \pm 4 \%$ and $T = 293 \pm 2 \text{ K}$. The error bars
 626 represent two standard deviations of the propagated error in the gradient of the k' against
 627 surface area graphs. See text for details.

628



629

630 **Figure 7.** The pseudo-first order rate constants as a function of aerosol surface area for copper
 631 (II) doped ammonium sulfate aerosols (black, shown in all panels) and with (a) malonic acid
 632 (blue), (b) citric acid (green), (c) 1,2 diaminoethane (orange), (d) tartronic acid (dark yellow)
 633 and (e) oxalic acid (red) added. The open coloured symbols represent a 2:1 molar ratio of the
 634 organic to the copper and the closed coloured symbols represent a 10:1 molar ratio of the
 635 organic to the copper. All experiments were performed at $RH = 60 \pm 3 \%$ and $T = 293 \pm 2 \text{ K}$.
 636 The error bars represent one standard deviation.

637

638

639 **References**

640

641 1. Brune, W. H.; Tan, D.; Faloon, I. F.; Jaegle, L.; Jacob, D. J.; Heikes, B. G.; Snow, J.; Kondo,
642 Y.; Shetter, R.; Sachse, et al., OH and HO₂ chemistry in the North Atlantic free troposphere. *Geophys.*
643 *Res. Lett.* **1999**, *26*, 3077-3080.

644 2. Cantrell, C. A.; Shetter, R. E.; Gilpin, T. M.; Calvert, J. G., Peroxy radicals measured during
645 Mauna Loa observatory photochemistry experiment 2: The data and first analysis. *J. Geophys. Res. -*
646 *Atmos.* **1996**, *101*, 14643-14652.

647 3. Carslaw, N.; Creasey, D. J.; Heard, D. E.; Jacobs, P. J.; Lee, J. D.; Lewis, A. C.; McQuaid, J.
648 B.; Pilling, M. J.; Bauguutte, S.; Penkett, et al., G., Eastern Atlantic Spring Experiment 1997 (EASE97)
649 - 2. Comparisons of model concentrations of OH, HO₂, and RO₂ with measurements. *J. Geophys. Res.*
650 *- Atmos.* **2002**, *107*, ACH 5.

651 4. Carslaw, N.; Creasey, D. J.; Heard, D. E.; Lewis, A. C.; McQuaid, J. B.; Pilling, M. J.; Monks,
652 P. S.; Bandy, B. J.; Penkett, S. A., Modeling OH, HO₂, and RO₂ radicals in the marine boundary layer
653 - 1. Model construction and comparison with field measurements. *J. Geophys. Res. - Atmos.* **1999**, *104*,
654 30241-30255.

655 5. Haggerstone, A. L.; Carpenter, L. J.; Carslaw, N.; McFiggans, G., Improved model predictions
656 of HO₂ with gas to particle mass transfer rates calculated using aerosol number size distributions. *J.*
657 *Geophys. Res. - Atmos.* **2005**, *110*, D04304.

658 6. Jaegle, L.; Jacob, D. J.; Brune, W. H.; Faloon, I.; Tan, D.; Heikes, B. G.; Kondo, Y.; Sachse,
659 G. W.; Anderson, B.; Gregory, et al., Photochemistry of HO_x in the upper troposphere at northern
660 midlatitudes. *J. Geophys. Res. - Atmos.* **2000**, *105*, 3877-3892.

661 7. Kanaya, Y.; Cao, R.; Kato, S.; Miyakawa, Y.; Kajii, Y.; Tanimoto, H.; Yokouchi, Y.; Mochida,
662 M.; Kawamura, K.; Akimoto, H., Chemistry of OH and HO₂ radicals observed at Rishiri Island, Japan,
663 in September 2003: Missing daytime sink of HO₂ and positive nighttime correlations with
664 monoterpene. *J. Geophys. Res. - Atmos.* **2007**, *112*, D11308.

665 8. Kanaya, Y.; Sadanaga, Y.; Matsumoto, J.; Sharma, U. K.; Hirokawa, J.; Kajii, Y.; Akimoto,
666 H., Daytime HO₂ concentrations at Oki Island, Japan, in summer 1998: Comparison between
667 measurement and theory. *J. Geophys. Res. - Atmos.* **2000**, *105*, 24205-24222.

668 9. Mao, J.; Jacob, D. J.; Evans, M. J.; Olson, J. R.; Ren, X.; Brune, W. H.; St Clair, J. M.; Crouse,
669 J. D.; Spencer, K. M.; Beaver, et al., Chemistry of hydrogen oxide radicals (HO_x) in the Arctic
670 troposphere in spring. *Atmos. Chem. Phys.* **2010**, *10*, 5823-5838.

671 10. Smith, S. C.; Lee, J. D.; Bloss, W. J.; Johnson, G. P.; Ingham, T.; Heard, D. E., Concentrations
672 of OH and HO₂ radicals during NAMBLEX: measurements and steady state analysis. *Atmos. Chem.*
673 *Phys.* **2006**, *6*, 1435-1453.

674 11. Sommariva, R.; Bloss, W. J.; Brough, N.; Carslaw, N.; Flynn, M.; Haggerstone, A. L.; Heard,
675 D. E.; Hopkins, J. R.; Lee, J. D.; Lewis, et al., OH and HO₂ chemistry during NAMBLEX: roles of
676 oxygenates, halogen oxides and heterogeneous uptake. *Atmos. Chem. Phys.* **2006**, *6*, 1135-1153.

677 12. Sommariva, R.; Haggerstone, A. L.; Carpenter, L. J.; Carslaw, N.; Creasey, D. J.; Heard, D. E.;
678 Lee, J. D.; Lewis, A. C.; Pilling, M. J.; Zador, J., OH and HO₂ chemistry in clean marine air during
679 SOAPEX-2. *Atmos. Chem. Phys.* **2004**, *4*, 839-856.

- 680 13. Stevens, P. S.; Mather, J. H.; Brune, W. H., Measurement of tropospheric OH and HO₂ by laser
681 induced fluorescence at low pressure. *J. Geophys. Res. - Atmos.* **1994**, *99*, 3543-3557.
- 682 14. Stone, D.; Whalley, L. K.; Heard, D. E., Tropospheric OH and HO₂ radicals: field
683 measurements and model comparisons. *Chem. Soc. Rev.* **2012**, *41*, 6348-6404.
- 684 15. Whalley, L. K.; Furneaux, K. L.; Goddard, A.; Lee, J. D.; Mahajan, A.; Oetjen, H.; Read, K.
685 A.; Kaaden, N.; Carpenter, L. J.; Lewis, A. C.; et al., The chemistry of OH and HO₂ radicals in the
686 boundary layer over the tropical Atlantic Ocean. *Atmos. Chem. Phys.* **2010**, *10*, 1555-1576.
- 687 16. Olson, J. R.; Crawford, J. H.; Brune, W.; Mao, J.; Ren, X.; Fried, A.; Anderson, B.; Apel, E.;
688 Beaver, M.; Blake, D.; et al., An analysis of fast photochemistry over high northern latitudes during
689 spring and summer using in-situ observations from ARCTAS and TOPSE. *Atmos. Chem. Phys.* **2012**,
690 *12*, 6799-6825.
- 691 17. de Reus, M.; Fischer, H.; Sander, R.; Gros, V.; Kormann, R.; Salisbury, G.; Van Dingenen, R.;
692 Williams, J.; Zöllner, M.; Lelieveld, J., Observations and model calculations of trace gas scavenging in
693 a dense Saharan dust plume during MINATROC. *Atmos. Chem. Phys.* **2005**, *5*, 1787-1803.
- 694 18. George, I. J.; Matthews, P. S. J.; Whalley, L. K.; Brooks, B.; Goddard, A.; Baeza-Romero, M.
695 T.; Heard, D. E., Measurements of uptake coefficients for heterogeneous loss of HO₂ onto submicron
696 inorganic salt aerosols. *Phys. Chem. Chem. Phys.* **2013**, *15*, 12829-12845.
- 697 19. Mozurkewich, M.; McMurry, P. H.; Gupta, A.; Calvert, J. G., Mass accommodation coefficient
698 for HO₂ Radicals on aqueous particles. *J. Geophys. Res. - Atmos.* **1987**, *92*, 4163-4170.
- 699 20. Taketani, F.; Kanaya, Y.; Akimoto, H., Kinetics of heterogeneous reactions of HO₂ radical at
700 ambient concentration levels with (NH₄)₂SO₄ and NaCl aerosol particles. *J. Phys. Chem. A* **2008**, *112*,
701 2370-2377.
- 702 21. Thornton, J.; Abbatt, J. P. D., Measurements of HO₂ uptake to aqueous aerosol: Mass
703 accommodation coefficients and net reactive loss. *J. Geophys. Res. - Atmos.* **2005**, *110*, D08309.
- 704 22. Jacob, D. J., Heterogeneous chemistry and tropospheric ozone. *Atmos. Env.* **2000**, *34*, 2131-
705 2159.
- 706 23. Mao, J.; Fan, S.; Jacob, D. J.; Travis, K. R., Radical loss in the atmosphere from Cu-Fe redox
707 coupling in aerosols. *Atmos. Chem. Phys.* **2013**, *13*, 509-519.
- 708 24. Ross, H. B.; Noone, K. J., A numerical investigation of the destruction of peroxy radical by Cu
709 ion catalyzed-reactions on atmospheric particles. *J. Atmos. Chem.* **1991**, *12*, 121-136.
- 710 25. Thornton, J. A.; Jaegle, L.; McNeill, V. F., Assessing known pathways for HO₂ loss in aqueous
711 atmospheric aerosols: Regional and global impacts on tropospheric oxidants. *J. Geophys. Res. - Atmos.*
712 **2008**, *113*, D05303.
- 713 26. Zhang, Q.; Jimenez, J. L.; Canagaratna, M. R.; Allan, J. D.; Coe, H.; Ulbrich, I.; Alfarra, M.
714 R.; Takami, A.; Middlebrook, A. M.; Sun, Y. L.; et al., Ubiquity and dominance of oxygenated species
715 in organic aerosols in anthropogenically-influenced northern hemisphere midlatitudes. *Geophys. Res.*
716 *Lett.* **2007**, *34*, L13801.
- 717 27. Murphy, D. M.; Cziczo, D. J.; Froyd, K. D.; Hudson, P. K.; Matthew, B. M.; Middlebrook, A.
718 M.; Peltier, R. E.; Sullivan, A.; Thomson, D. S.; Weber, R. J., Single-particle mass spectrometry of
719 tropospheric aerosol particles. *J. Geophys. Res. - Atmos.* **2006**, *111*, D23S32.

- 720 28. Vonpichowski, M.; Nauser, T.; Hoigne, J.; Buhler, R. E., O₂⁻ decay catalyzed by Cu²⁺ and Cu⁺
721 ions in aqueous solutions - a pulse radiolysis study for atmospheric chemistry. *Phys. Chem. Chem. Phys.*
722 **1993**, *97*, 762-771.
- 723 29. Okochi, H.; Brimblecombe, P., Potential trace metal-organic complexation in the atmosphere.
724 *Scientific World J.* **2002**, *2*, 767-86.
- 725 30. Taketani, F.; Kanaya, Y.; Pochanart, P.; Liu, Y.; Li, J.; Okuzawa, K.; Kawamura, K.; Wang,
726 Z.; Akimoto, H., Measurement of overall uptake coefficients for HO₂ radicals by aerosol particles
727 sampled from ambient air at Mts. Tai and Mang (China). *Atmos. Chem. Phys.* **2012**, *12*, 11907-11916.
- 728 31. Heard, D. E.; Pilling, M. J., Measurement of OH and HO₂ in the troposphere. *Chem. Rev.* **2003**,
729 *103*, 5163-5198.
- 730 32. Clegg, S. L.; Brimblecombe, P.; Wexler, A. S., Thermodynamic model of the system
731 H⁺-NH₄⁺-Na⁺-SO₄²⁻-NO₃⁻-Cl⁻-H₂O at 298.15 K. *J. Phys. Chem. A* **1998**, *102*, 2155-2171.
- 732 33. Wexler, A. S.; Clegg, S. L., Atmospheric aerosol models for systems including the ions H⁺,
733 NH₄⁺, Na⁺, SO₄²⁻, NO₃⁻, Cl⁻, Br⁻, and H₂O. *J. Geophys. Res. - Atmos.* **2002**, *107*, 4207.
- 734 34. Brown, R. L., Tubular flow reactors with 1st-order kinetics. *J. Res. Nat. Bur. Stand.* **1978**, *83*,
735 1-8.
- 736 35. Fuchs, N. A.; Sutagin, A. G., Properties of highly dispersed aerosols. Ann Arbor Science
737 Publishers: Ann Arbor, MI, 1970.
- 738 36. Kieber, R. J.; Skrabal, S. A.; Smith, C.; Willey, J. D., Redox speciation of copper in rainwater:
739 Temporal variability and atmospheric deposition. *Environ. Sci. Technol.* **2004**, *38*, 3587-3594.
- 740 37. Shank, G. C.; Skrabal, S. A.; Whitehead, R. F.; Kieber, R. J., Strong copper complexation in
741 an organic-rich estuary: the importance of allochthonous dissolved organic matter. *Mar. Chem.* **2004**,
742 *88*, 21-39.
- 743 38. Christl, I.; Kretzschmar, R., Interaction of copper and fulvic acid at the hematite-water
744 interface. *Geochim. Cosmochim. Ac.* **2001**, *65*, 3435-3442.
- 745 39. Flaschka, H. A., *EDTA Titrations: An introduction to theory and practice*. Pergamon Press:
746 New York, 1959.
- 747 40. Schwartz, S. E., Mass-transport considerations pertinent to aqueous phase reactions of gases in
748 liquid-water clouds. *Jaeschke, W. (Ed.) Nato ASI (Advanced Science Institute Series Series G*
749 *Ecological Sciences), Vol. 6. Chemistry of Multiphase Atmospheric Systems; Symposium, Corfu,*
750 *Greece, Sept. 26-Oct. 8, 1983. Xvi+773p. Springer-Verlag: Berlin, West Germany; New York, N.Y.,*
751 *USA. Illus* **1986**, 415-472.
- 752 41. Badger, C. L.; Griffiths, P. T.; George, I.; Abbatt, J. P. D.; Cox, R. A., Reactive uptake of N₂O₅
753 by aerosol particles containing mixtures of humic acid and ammonium sulfate. *J. Phys. Chem. A* **2006**,
754 *110*, 6986-6994.
- 755 42. Thornton, J. A.; Abbatt, J. P. D., N₂O₅ reaction on submicron sea salt aerosol: Kinetics,
756 products, and the effect of surface active organics. *J. Phys. Chem. A* **2005**, *109*, 10004-10012.
- 757 43. Lakey, P. S. J.; George, I. J.; Whalley, L. K.; Baeza-Romero, M. T.; Heard, D. E.,
758 Measurements of the HO₂ uptake coefficients onto single component organic aerosols. *Environ Sci*
759 *Technol* **2015**, *49*, 4878-4885.

- 760 44. Shiraiwa, M.; Pfrang, C.; Pöschl, U., Kinetic multi-layer model of aerosol surface and bulk
761 chemistry (KM-SUB): the influence of interfacial transport and bulk diffusion on the oxidation of oleic
762 acid by ozone. *Atmos. Chem. Phys.* **2010**, *10*, 3673-3691.
- 763 45. Zhou, S. M.; Shiraiwa, M.; McWhinney, R. D.; Poschl, U.; Abbatt, J. P. D., Kinetic limitations
764 in gas-particle reactions arising from slow diffusion in secondary organic aerosol. *Faraday Discuss.*
765 **2013**, *165*, 391-406.
- 766 46. Drozd, G.; Woo, J.; Häkkinen, S. A. K.; Nenes, A.; McNeill, V. F., Inorganic salts interact with
767 organic di-acids in sub-micron particles to form material with low hygroscopicity and volatility. *Atmos.*
768 *Chem. Phys.* **2013**, *14*, 5205-5215.
- 769 47. Fu, P.; Kawamura, K.; Usukura, K.; Miura, K., Dicarboxylic acids, ketocarboxylic acids and
770 glyoxal in the marine aerosols collected during a round-the-world cruise. *Mar. Chem.* **2013**, *148*, 22-
771 32.
- 772 48. Myriokefalitakis, S.; Tsigaridis, K.; Mihalopoulos, N.; Sciare, J.; Nenes, A.; Kawamura, K.;
773 Segers, A.; Kanakidou, M., In-cloud oxalate formation in the global troposphere: a 3-D modeling study.
774 *Atmos. Chem. Phys.* **2011**, *11*, 5761-5782.
- 775 49. Neusüss, C.; Pelzing, M.; Plewka, A.; Herrmann, H., A new analytical approach for size-
776 resolved speciation of organic compounds in atmospheric aerosol particles: Methods and first results.
777 *J. Geophys. Res. - Atmos.* **2000**, *105*, 4513-4527.
- 778 50. Mueller, K.; Lehmann, S.; van Pinxteren, D.; Gnauk, T.; Niedermeier, N.; Wiedensohler, A.;
779 Herrmann, H., Particle characterization at the Cape Verde atmospheric observatory during the 2007
780 RHaMBLe intensive. *Atmos. Chem. Phys.* **2010**, *10*, 2709-2721.
- 781 51. Fomba, K. W.; Müller, K.; van Pinxteren, D.; Herrmann, H., Aerosol size-resolved trace metal
782 composition in remote northern tropical Atlantic marine environment: case study Cape Verde islands.
783 *Atmos. Chem. Phys.* **2013**, *13*, 4801-4814.
- 784 52. Lee, J. D.; McFiggans, G.; Allan, J. D.; Baker, A. R.; Ball, S. M.; Benton, A. K.; Carpenter, L.
785 J.; Commane, R.; Finley, B. D.; Evans, et al., Reactive Halogens in the Marine Boundary Layer
786 (RHaMBLe): the tropical North Atlantic experiments. *Atmos. Chem. Phys.* **2010**, *10*, 1031-1055.
- 787 53. Carpenter, L. J.; Fleming, Z. L.; Read, K. A.; Lee, J. D.; Moller, S. J.; Hopkins, J. R.; Purvis,
788 R. M.; Lewis, A. C.; Müller, K.; Heinold, B.; et al., Seasonal characteristics of tropical marine boundary
789 layer air measured at the Cape Verde Atmospheric Observatory. *J. Atmos. Chem.* **2010**, *67*, 87-140.
- 790 54. Matthews, P. S. J.; Baeza-Romero, M. T.; Whalley, L. K.; Heard, D. E., Uptake of HO₂ radicals
791 onto Arizona test dust particles using an aerosol flow tube. *Atmos. Chem. Phys.* **2014**, *14*, 7397-7408.

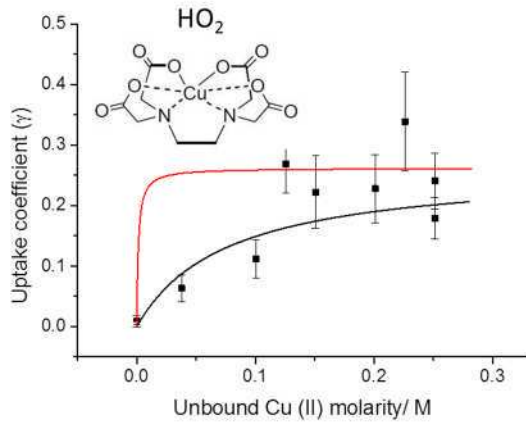
792

793

794

795 **Table of Contents Image**

796



797

798

799

800

801

802

803

804

805

806

807

808

809